

COMPLEX SYSTEMS

This topic looks at systems that are more complex than those described in Chapters 3 to 5 in *Environmental Biotechnology*. Complexity comes about in two ways. The first is when the system is *not at steady state*. Then, the various components in the system—for example, the active biomass, the inert biomass, the substrate, and the soluble microbial products—behave quite differently. Overall system performance under nonsteady-state conditions is quite dynamic, and sometimes it is counterintuitive. The second type of complexity occurs when distinctly different types of microorganisms comprise a *multispecies system*. The principles of microbial ecology (Chapter 1) apply as the different microbial types interact with each other and their environment.

Here, we develop and apply advanced tools to quantify these more complex systems. We begin with nonsteady-state conditions, where we explore how the different components respond in suspended-growth and biofilm systems. Then, we utilize an important example of a multispecies system—aerobic heterotrophs and nitrifiers—to understand how to quantify their interactions and how those interactions can affect process performance.

NONSTEADY-STATE SYSTEMS

Although many bioreactor systems employed in environmental biotechnology are at or very close to steady state, some systems experience nonsteady-state, or time-varying, conditions. The classic example of a nonsteady-state process is the batch reactor. Fed-batch, fill-and-draw, and sequencing-batch systems are obvious examples of reactor systems having significant time-varying conditions. Nonsteady-state conditions also can occur for continuously fed processes when:

- The substrate loading experiences substantial and prolonged changes
- Environmental conditions, such as temperature, are altered
- Operating conditions, such as the SRT, change
- An inhibitory substance is introduced
- The biomass moves or cycles between locations that have markedly different growth conditions

The major difference between steady-state and nonsteady-state systems is that the concentrations of substrates, products, and biomass can change with time. While the phenomena and their rate expressions, described in the previously mentioned Chapters 3 through 5, continue to be valid, the most important difference for representing nonsteady-state conditions is that the accumulation terms, for example, $V(dS/dt)$, $V(dX_a/dt)$, $V(dX_v/dt)$, and $V(dUAP/dt)$, are no longer automatically set to zero. Generally, the concentrations to which the microorganisms are exposed within a biofilm or a floc quickly reach steady state with respect to the bulk-liquid concentrations. Hence, the nonzero accumulation terms usually are those in the bulk liquid.

Because all of the modeled variables can change with time, a solution algorithm must “march forward” from some initial conditions. Because the nonsteady-state differential equations are nonlinear and coupled, the most effective (and usually only) solution algorithm is a numerical method, in which time is broken into small Δt increments. The simplest numerical scheme is a *forward method*, in which the value of a variable is augmented by the change computed from the nonsteady-state mass balance and all concentrations at the start of the current time step.

The forward method is illustrated for the substrate in a chemostat:

$$S(t + \Delta t) = S(t) + \frac{dS(t)}{dt} \Delta t \quad [1]$$

in which $S(t)$ is the substrate concentration at the start of the current time, $S(t + \Delta t)$ is the substrate concentration for Δt to the future, and $dS(t)/dt$ is computed from Equation 2 with concentrations for the current time,

$$\frac{dS(t)}{dt} = -\frac{\hat{q}(t)S(t)}{K(t) + S(t)} X_a(t) + \frac{Q(t)}{V(t)} (S^0(t) - S(t)) \quad [2]$$

In Equation 2, all concentrations and parameters have the same definition as in Chapter 3 and are written as having time dependency. This means that the solution algorithm must augment or update all concentrations and variables for each time step. The concentrations in the reactor are augmented by equation sets of the form of Equations 1 plus 2. Some parameter values also must be updated. For example, a change in substrate loading would be reflected in updated values of $S^0(t)$ and/or $Q(t)$, while a change in temperature would alter $\hat{q}(t)$, $b(t)$, and other rate parameters.

The concept underlying numerical solutions is that Δt should be small enough that the concentration changes occurring in Δt are small and do not cause significant errors in the computed differentials, such as Equation 2. In most cases of continuously fed processes, substrate concentrations change most rapidly and control the size of Δt . For batch processes in which the biomass starts with a small inoculum, active biomass may control Δt . In any case, selecting small enough time steps precludes errors or instability. In general, Δt is small enough when $(d\psi(t)/dt)\Delta t \ll \psi(t)$, in which $\psi(t)$ represents any of the variables being tracked by the model. Over the long term, or many Δt s, the $\psi(t)$ values can change dramatically and in accord with the nonsteady-state mass balances, even though their changes in any one time step are small. Basic reactor systems such as chemostats or completely mixed biofilm reactors

can be solved in a straightforward manner with spreadsheets or commercial software, such as MATHCAD or Mathematica. Sophisticated solver programs, reviewed by Press, Flannery, Teukolsky, and Vetterling (1986) and Steefel and MacQuarrie (1996), are available for more complicated configurations and when the number of variables becomes larger, situations in which maximizing computational efficiency is necessary.

EXAMPLES OF NONSTEADY-STATE SYSTEMS

A set of examples illustrates how the nonsteady-state mass balances are put together and solved to yield insights into settings of importance to environmental biotechnology. Since these examples are illustrative of modeling methods and generalized trends, a set of standard conditions is imposed. These conditions are for the aerobic biodegradation of an organic electron donor (expressed as BOD_L or biodegradable COD). Consistent with Chapters 3 through 4, the examples describe a rate-limiting electron-donor substrate (S), active biomass (X_a), inert biomass (X_i), substrate-utilization-associated products (UAP), and biomass-associated products (BAP). Unless noted otherwise, oxygen is assumed to be nonlimiting and is not modeled.

Table 1 lists the standard parameter values used for these examples. The temperature that corresponds to these values is 20 °C. Additional parameters or changes are given when needed.

The examples are solved by “marching forward” in time for all variables included in the example. Initial conditions, flows, input concentrations, and any special factors

Table 1 Standard parameter values used in nonsteady-state examples

Parameter	Value	Units
\hat{q}	10	mg BOD_L /mg VSS_a -d
K	20	mg BOD_L /l
\hat{q}_{UAP}	1.8	mg COD_P /mg VSS_a -d
K_{UAP}	100	mg COD_P /l
\hat{q}_{BAP}	0.1	mg COD_P /mg VSS_a -d
K_{BAP}	85	mg COD_P /l
k_1	0.12	mg COD_P /mg BOD_L
k_2	0.09	mg COD_P /mg VSS_a -d
b	0.15	d ⁻¹
f_d	0.8	—
Y	0.42	mg VSS_a /mg BOD_L
D	1.0	cm ² /d
D_f	0.8	cm ² /d
X_f	40	mg VSS_a /cm ³
L	50 (5×10^{-3})	μ m (cm)

are specified for each example. From the initial conditions, each variable (denoted by ψ in general) is updated for each step by using an equation of the form of Equation 1. The values of all variables and parameters at the current time step are used to compute $d\psi(t)/dt$, which is then combined with $\psi(t)$ and Δt to yield the value at the next time step, $\psi(t + \Delta t)$.

The examples begin with very simple ones that include only the most basic phenomena. These simple examples illustrate how the nonsteady-state models are set-up and solved. Continuing examples increase the number of variables included and the complexity of the reactor setting. The dynamic nature of the nonsteady-state situation requires that the effects of SMP generation and biodegradation be described in a more sophisticated manner than was used in Chapters 3 and 4; how to handle SMP in the nonsteady-state setting is described beginning with the third example.

Example 1

BATCH GROWTH FROM A SMALL INOCULUM Batch growth is commonly used to grow biomass from a small inoculum. It serves as an excellent example of the most basic features on nonsteady-state modeling. Chapter 5 gave the basic set-up for a batch reactor, but several simplifying assumptions were needed to obtain an analytical solution. Here, we use a numerical method and do not need so many simplifications.

For this example, only the rate-limiting substrate and the active biomass are represented. The following initial conditions are specified:

$$\begin{aligned} X_a^{\text{in}} &= 0.1 \text{ mg VSS}_a/\text{l (approximately } 10^9 \text{ cells/l)} \\ S^{\text{in}} &= 1,000 \text{ mg BOD}_L/\text{l} \end{aligned}$$

For batch operation, $Q = 0$, while V is constant.

Nonsteady-state mass balances are required for S and X_a . They are

$$V \frac{dS}{dt} = QS^0 - QS - \frac{\hat{q}S}{K+S} X_a V \quad [3]$$

which simplifies to

$$\frac{dS}{dt} = -\frac{\hat{q}S}{K+S} X_a \quad [4]$$

and

$$V \frac{dX_a}{dt} = QX_a^0 - QX_a + Y \frac{\hat{q}S}{K+S} X_a V - bX_a V \quad [5]$$

which simplifies to

$$\frac{dX_a}{dt} = Y \frac{\hat{q}S}{K+S} X_a - bX_a = Y \left(-\frac{dS}{dt} \right) - bX_a \quad [6]$$

The solution marches forward in time according to

$$S(t + \Delta t) = S(t) + \frac{dS(t)}{dt} \Delta t \quad [7]$$

and

$$X_a(t + \Delta t) = X_a(t) + \frac{dX_a(t)}{dt} \Delta t \quad [8]$$

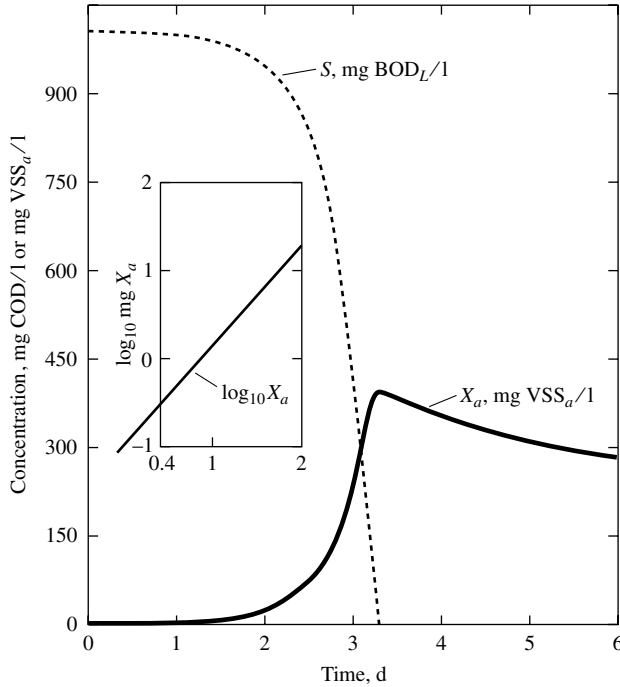


Figure 1 Time course for S and X_a in the batch reaction of Example 1. The inset shows the logarithmic growth from a very small inoculum in the first 2 days.

The values of $S(t)$ and $X_a(t)$ are substituted into Equations 4 and 6 to obtain the differentials at time = t .

To exemplify the “marching forward” approach, we compute the new values of S and X_a for the first time step. Initial conditions give:

$$\frac{dS}{dt} = -\frac{10 \text{ mg BOD}_L/\text{mg VSS}_a - d \cdot 1,000 \text{ mg BOD}_L/\text{l}}{(20 + 1,000) \text{ mg BOD}_L/\text{l}} \cdot \frac{0.1 \text{ mg VSS}_a}{1} = -0.98 \frac{\text{mg BOD}_L}{1 - d}$$

Then, with $\Delta t = 0.01$ d,

$$S(0.01 \text{ d}) = 1,000 - 0.98 \cdot 0.01 = 999.99 \text{ mg BOD}_L/\text{l}$$

$$\frac{dX_a}{dt} = 0.42 \frac{\text{mg VSS}_a}{\text{mg BOD}_L} \cdot \frac{0.98 \text{ mg BOD}_L}{1 - d} - (0.15/\text{d}) \cdot 0.1 \text{ mg VSS}_a/\text{l} = 0.397 \frac{\text{mg VSS}_a}{1 - d}$$

$$X_a(0.01 \text{ d}) = 0.1 + 0.397 \cdot 0.01 = 0.10397 \text{ mg VSS}_a/\text{l}$$

Figure 1 presents the results for continuing these calculations over time S and X_a . As is normal for batch growth, an apparent “lag phase” occurs as the biomass concentration grows from a very small inoculum to a concentration large enough to decrease the substrate concentration by a detectable amount. Subsequently, biomass growth and substrate depletion occur rapidly and in parallel (the “log-growth” phase) until the substrate is nearly depleted. Then, the biomass reaches a peak, often called the “stationary phase.” Finally, the active biomass slowly declines in concentration due to decay.

Example 2

APPROACH TO STEADY-STATE IN A CHEMOSTAT The rate-limiting substrate, active biomass, and inert biomass are allowed to approach their steady-state levels in a chemostat of volume $V = 1000 \text{ m}^3$ and with a steady feed of:

$$Q = 1,000 \text{ m}^3/\text{d}$$

$$S^0 = 1,000 \text{ mg BOD}_L/\text{l}$$

$$X_i^0 = X_a^0 = 0$$

and a small starting inoculum of $X_a^{\text{in}} = 0.1 \text{ mg VSS}_a/\text{l}$ and $S^{\text{in}} = 1,000 \text{ mg BOD}_L/\text{l}$. The mass balances and differential equations are:

$$V \frac{dS}{dt} = QS^0 - QS - \frac{\hat{q}S}{K+S} X_a V \quad [9]$$

$$V \frac{dX_a}{dt} = QX_a^0 - QX_a + Y \frac{\hat{q}S}{K+S} X_a V - bX_a V \quad [10]$$

$$V \frac{dX_i}{dt} = QX_i^0 - QX_i + (1 - f_d)bX_a V \quad [11]$$

which simplify to

$$\frac{dS}{dt} = \frac{Q}{V}(S^0 - S) - \frac{\hat{q}S}{K+S} X_a \quad [12]$$

$$\frac{dX_a}{dt} = -\frac{Q}{V} X_a + \left(Y \frac{\hat{q}S}{K+S} - b \right) X_a \quad [13]$$

$$\frac{dX_i}{dt} = -\frac{Q}{V} X_i + (1 - f_d)bX_a \quad [14]$$

Equations 12 to 14 are solved by marching forward from initial conditions ($X_a^{\text{in}} = 0.1 \text{ mg VSS}_a/\text{l}$ and $S^{\text{in}} = 1,000 \text{ mg BOD}_L/\text{l}$). The marching-forward technique uses the format of Equation 1, as illustrated in Example 1.

Figure 2 presents the nonsteady-state results. Similar to the batch reactor, there are apparent log, log-growth, and stationary phases when the starting inoculum is small. The absolute time required to reach the log phase is longer than for strictly batch growth (Figure 1), because advective loss of biomass ($[-Q/V]X_a$ in Equation 13) slows the net accumulation rate. A declining phase does not occur, since fresh substrate is continuously provided by the feed ($[Q/V]S^0$ in Equation 12), which means that S is not driven to zero, but remains at its steady-state value of 15.2 mg/l. Thus, the chemostat comes to a true steady state, in which new synthesis is balanced by decay and advection. Because it is the “slowest growing” species, inert biomass is at a much lower concentration than active biomass when the steady-state specific growth rate ($\mu = D = Q/V$) is fast, 1/d in this case.

Example 3

BATCH GROWTH WHEN SMP IS CONSIDERED The previous examples illustrate the most basic trends when substrate is amply available. When substrate supply is more limited—the more usual condition in nature, in continuous treatment processes, and after substrate is depleted in a batch reaction—soluble microbial products become important. The dynamic nature of nonsteady-state systems and the highly different kinetics among original substrate, UAP, and BAP require that their effects be handled in a more sophisticated manner than is necessary for steady-state systems.

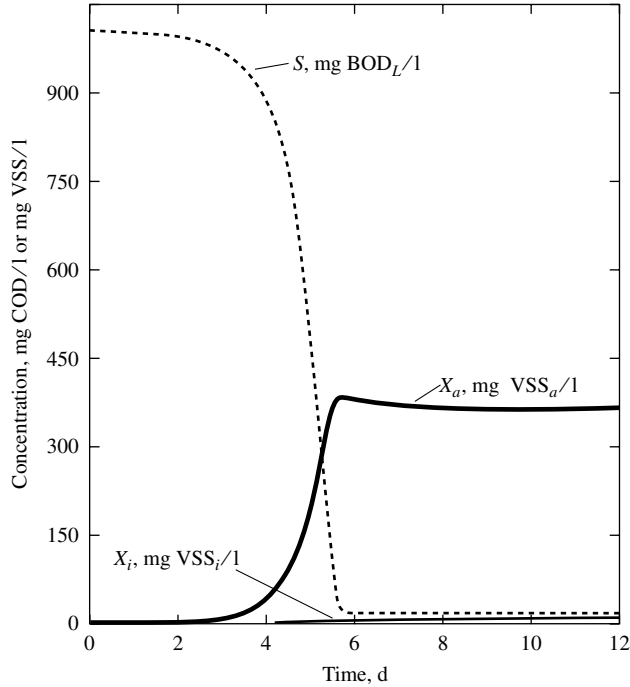


Figure 2 The gradual approach to steady state for a chemostat started from a small inoculum and fed continuously at $Q/V = 1/d$ and $S^0 = 1,000$ mg BOD_L/l .

In this example, batch-growth conditions are:

- $V = 1$ liter
- $S^{in} = 1,000$ mg BOD_L/l
- $UAP^{in} = BAP^{in} = 0$
- $X_a^{in} = 0.1$ mg VSS_a/l
- $X_i^{in} = 0$

The mass-balance equations, written directly in the differential format, are as follows. For substrate,

$$\frac{dS}{dt} = -\frac{\hat{q}S}{K + S} X_a \tag{15}$$

is the same as in Example 1. UAP and BAP are generated and consumed by the same mechanisms as were described in Chapter 3:

$$\frac{d UAP}{dt} = k_1 \frac{\hat{q}S}{K + S} X_a - \frac{\hat{q}UAP}{K_{UAP} + UAP} X_a \tag{16}$$

$$\frac{d BAP}{dt} = k_2 X_a - \frac{\hat{q}BAP}{K_{BAP} + BAP} X_a \tag{17}$$

In the nonsteady-state system, active biomass is synthesized through utilization of original substrate and SMP, while it is lost through endogenous decay and formation of BAP:

$$\frac{dX_a}{dt} = Y \left(\frac{\hat{q}S}{K+S} + \frac{\hat{q}_{UAP} UAP}{K_{UAP} + UAP} + \frac{\hat{q}_{BAP} BAP}{K_{BAP} + BAP} \right) X_a - (b + k_2/1.42) X_a \quad [18]$$

The 1.42 factor converts the COD in the biomass to VSS, that is, 1.42 mg COD/mg VSS for $C_5H_7O_2N$. Equation 18 assumes that Y is the same for substrate and SMP. Finally, the X_i balance is

$$\frac{dX_i}{dt} = (1 - f_d) b X_a \quad [19]$$

Figure 3 presents the nonsteady-state results, which were obtained by the marching-forward technique in which Equations 15 to 19 were used to update the concentrations for each time step. Although the general trends for S and X_a are similar to those of Figure 1, several important differences are apparent. First, formation and consumption of UAP and BAP mean that the total soluble COD ($= S + UAP + BAP$) declines more slowly than S , has a “hump” when the UAP is highest, and ends up with a slowly increasing residual comprised of BAP. Figure 3 shows an extended stationary phase, during which UAP consumption gives new biomass synthesis. The residual SMP, as well as the biomass, are reservoirs for electron equivalents and explain why long-term BOD and BDOC (biodegradable dissolved organic carbon, discussed in Chapter 12) tests do not measure 100 percent of the original electron-donor substrate (Woolschlager and Rittmann, 1995). For instance, the oxygen consumed at the end of the batch incubation (6 days) can be computed from an oxygen-demand balance:

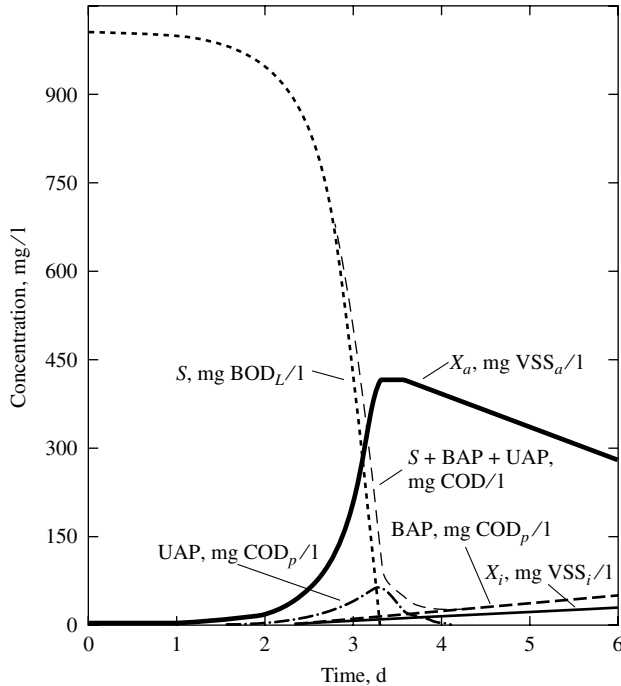


Figure 3 Time-dependent changes in S , X_a , X_i , UAP, and BAP for batch utilization of 1,000 mg BOD_L/l .

$$\begin{aligned} \text{O}_2 \text{ consumed} &= (S^{\text{in}} - S) + (\text{UAP}^{\text{in}} - \text{UAP}) + (\text{BAP}^{\text{in}} - \text{BAP}) \\ &\quad + 1.42(X_a^{\text{in}} + X_i^{\text{in}} - X_a - X_i) \\ &= (1,000 - 0) + (0 - 0) + (0 - 52) + 1.42(0.1 + 0 - 282 - 30) \\ &= 505 \text{ mg O}_2/\text{l} \end{aligned}$$

Thus, the complete removal of 1,000 mg/l of BOD_L results in a measured OD of 505 mg/l after 6 days of batch incubation. The same computation for $t = 5$ days yields what would be measured as the 5-day BOD, or

$$\text{BOD}_5 = (1,000 - 0) + (0 - 0.1) + (0 - 40) + 1.42(0.1 + 0 - 337 - 22) = 450 \text{ mg/l}$$

Thus, the 5-day BOD is 45 percent of the true or ultimate BOD of 1,000 mg/l in this case.

TRANSIENT LOADING CHANGES TO CHEMOSTAT: ALTERING Q AND θ_x

Example 4

A chemostat is initially operating at a steady-state condition of

$$\begin{aligned} V &= 1,000 \text{ m}^3 \\ Q &= 200 \text{ m}^3/\text{d} \\ S^0 &= 1,000 \text{ mg BOD}_L/\text{l} \\ X_a^0 &= 0 \text{ mg VSS}_a/\text{l} \\ X_i^0 &= 0 \text{ mg VSS}_i/\text{l} \\ \text{UAP}^0 &= \text{BAP}^0 = 0 \end{aligned}$$

It is then subjected to sudden step increase in flow to 400 m³/d. The system then achieves the new steady state. Twenty-five days later, Q is suddenly returned to 200 m³/d. Thus, this example halves and then doubles the SRT. The system is analyzed for S , X_a , X_i , UAP, and BAP.

The nonsteady-state mass balances, in differential format, are:

$$\frac{dS}{dt} = \frac{Q}{V}(S^0 - S) - \frac{\hat{q}S}{K + S}X_a \quad \text{[20]}$$

$$\frac{d \text{UAP}}{dt} = \frac{Q}{V}(-\text{UAP}) + k_1 \frac{\hat{q}S}{K + S}X_a - \frac{\hat{q}\text{UAP}\text{UAP}}{K_{\text{UAP}} + \text{UAP}}X_a \quad \text{[21]}$$

$$\frac{d \text{BAP}}{dt} = \frac{Q}{V}(-\text{BAP}) + k_2 X_a - \frac{\hat{q}\text{BAP} \text{BAP}}{K_{\text{BAP}} + \text{BAP}}X_a \quad \text{[22]}$$

$$\frac{dX_a}{dt} = \frac{Q}{V}(-X_a) + Y \left[\frac{\hat{q}S}{K + S} + \frac{\hat{q}\text{UAB} \text{UAP}}{K_{\text{UAP}} + \text{UAP}} + \frac{\hat{q}\text{BAP} \text{BAP}}{K_{\text{BAP}} + \text{BAP}} \right] X_a - (b + k_2/1.42)X_a \quad \text{[23]}$$

$$\frac{dX_i}{dt} = \frac{Q}{V}(-X_i) + (1 - f_d)bX_a \quad \text{[24]}$$

Figure 4 shows how the variables respond to the imposed changes in Q . As with all the prior examples, concentrations were updated by using the differential values (Equations 20 to 24). What is most insightful is seeing the relative time frames for the responses of the different variables. The variables tied directly to biomass—that is, X_a , X_i , and BAP—respond relatively slowly, but monotonically towards the new steady state. On the other hand, S and

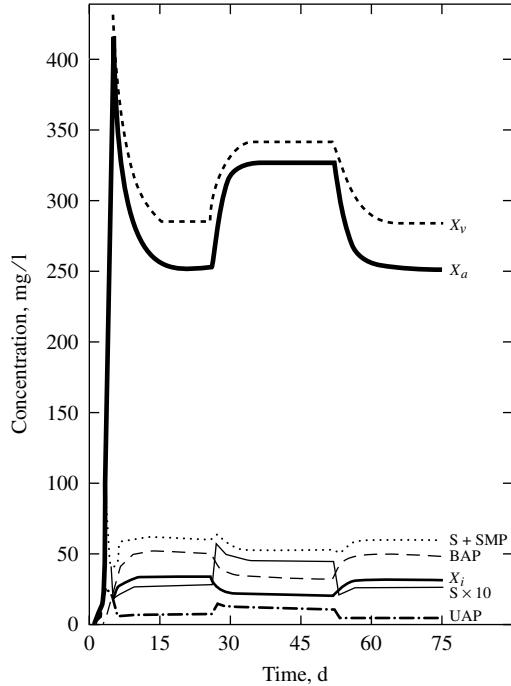


Figure 4 Response of the chemostat to Q and $\theta_x = \theta$ changes. The initial conditions have $S^0 = 1,000$ mg BOD_L/l and $\theta_x = 5$ d. At day 25, θ_x is changed to 2.5 d. At 50 d, θ_x is returned to 5 days.

UAP (which is produced directly from substrate utilization) respond quickly to Q changes, but then slowly return to steady-state levels as X_a adjusts to the new θ_x .

The sum of the soluble components ($S + BAP + UAP$) has a response pattern that most closely tracks BAP, which is its main component. However, the summed response is damped, because the long-term changes in S and UAP are counter to those of BAP. Thus, the soluble COD remains between 50 and 62 mg COD/l, even though the substrate loading is doubled or halved as the SRT varies by a factor of two. Likewise, X_v mainly follows X_a , but the response is dampened by X_i , which moves oppositely to X_a .

Example 5

TRANSIENT LOADING CHANGES TO A CHEMOSTAT: ALTERING S^0 The initial steady-state conditions of Example 4 are altered by a two-step change in S^0 : from 1,000 mg BOD_L/l to 2,000 mg BOD_L/l and back to 1,000 mg BOD_L/l. Equations 20 to 24 remain the relevant ones, and Figure 5 shows the results. An increase in substrate loading due to an increase in S^0 causes S and UAP to increase rapidly and then decline as X_a adjusts upward. BAP remains relatively stable and controls the soluble COD, which moves up or down in a gradual manner that tracks X_a .

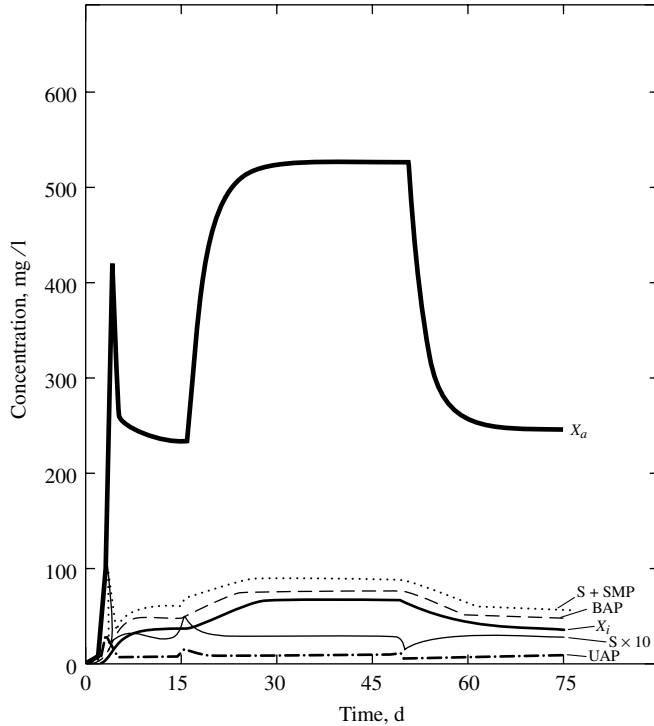


Figure 5 Response of a chemostat to S^0 changes. The initial loading has $S^0 = 1,000$ mg BOD_L/l and $\theta_x = \theta = 5$ d. At 15 days, S^0 is increased to 2,000 mg BOD_L/l, while it is returned to 1,000 mg/l at 50 days.

EFFECT OF A TEMPERATURE CHANGE ON THE PERFORMANCE OF A CHEMOSTAT

As before, the steady state of Example 5 is the starting condition. In this case, a sudden 10°C drop in temperature occurs, and the following kinetic parameters change:

\hat{q}	10 to 5	mg BOD _L /mg VSS _a - d
\hat{q}_{UAP}	1.8 to 0.9	mg COD _p /mg VSS _a - d
\hat{q}_{BAP}	0.1 to 0.05	mg COD _p /mg VSS _a - d
b	0.15 to 0.075	d ⁻¹
k_2	0.09 to 0.045	mg COD _p /mg VSS _a - d

All other parameters remain the same. Equations 20 to 24 describe the nonsteady-state conditions.

Figure 6 presents the effects of the sudden and dramatic temperature decrease. Initially, S, UAP, and the total soluble COD increase. In the long term, however, the total soluble COD and BAP decline, and this is caused by the gradual increase in active biomass, due to a reduced decay rate. The inert biomass gradually decreases because of the slower decay.

Example 6

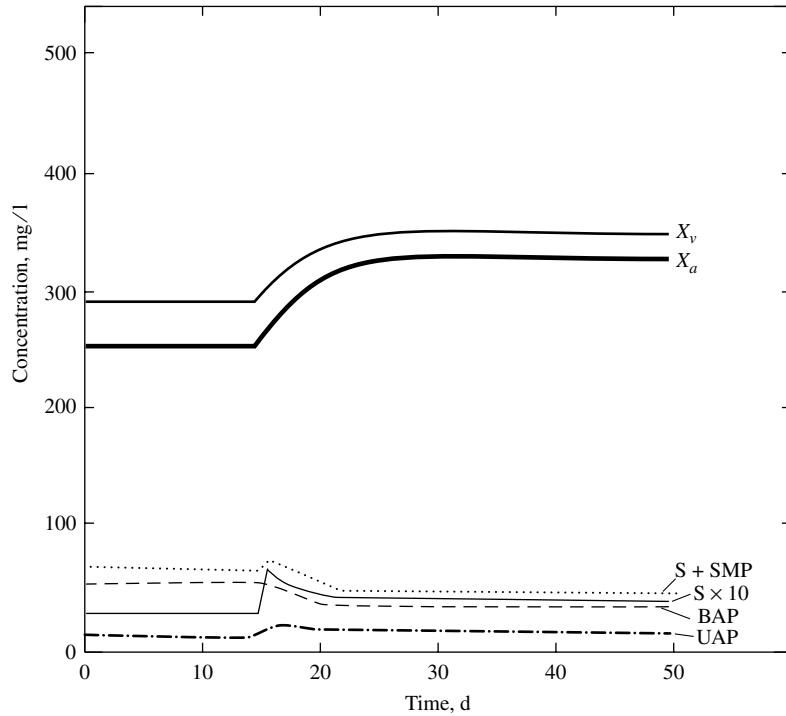


Figure 6 Effects of a sudden decrease in temperature in the chemostat. At day 15, the temperature suddenly drops from 20°C to 10°C.

Example 7

APPROACH TO STEADY STATE FOR A COMPLETELY MIXED BIOFILM REACTOR AND CONSIDERING SMP

Active and inactive biomasses in a biofilm accumulate in a manner similar to that for a chemostat when a small inoculum initiates growth. For this example, the conditions are:

$$hV = 1,000 \text{ m}^3$$

$$Q = 1,000 \text{ m}^3/\text{d}$$

$$S^0 = 1,000 \text{ mg BOD}_L/\text{l}$$

$$aV = 100,000 \text{ m}^2$$

$$a/h = 100 \text{ m}^{-1}$$

$$X_f L_f^{\text{in}} = 1 \text{ mg VSS}_a/\text{m}^2$$

$$X_{fi} L_f^{\text{in}} = 0 \text{ mg VSS}_i/\text{m}^2$$

$$b_{\text{det}} = 1/\text{d}$$

These conditions conform to a relatively high-load condition (recall the section on Normalized Surface Loading in Chapter 4), which should lead to a deep biofilm for steady-state conditions. The mass-balance equations are constructed by analogy to the equations in Example 4, but with the biofilm-process conversions described in the section on Completely Mixed Biofilm Reactors in Chapter 4:

$$\frac{dS}{dt} = \frac{Q}{hV}(S^0 - S) - Ja/h$$

[25]

$$\frac{d \text{UAP}}{dt} = -\frac{Q}{hV} \text{UAP} + k_1 J a/h - \frac{\hat{q}_{\text{UAP}} \text{UAP}}{K_{\text{UAP}} + \text{UAP}} X_f L_f a/h \quad [26]$$

$$\frac{d \text{BAP}}{dt} = -\frac{Q}{hV} \text{BAP} + k_2 X_f L_f a/h - \frac{\hat{q}_{\text{BAP}} \text{BAP}}{K_{\text{BAP}} + \text{BAP}} X_f L_f a/h \quad [27]$$

$$\frac{d X_f L_f}{dt} = Y J + Y \left(\frac{\hat{q}_{\text{UAP}} \text{UAP}}{K_{\text{UAP}} + \text{UAP}} + \frac{\hat{q}_{\text{BAP}} \text{BAP}}{K_{\text{BAP}} + \text{BAP}} \right) X_f L_f - (b + b_{\text{det}} + k_2/1.42) X_f L_f \quad [28]$$

$$\frac{d X_{fi} L_f}{dt} = (1 - f_d) b X_f L_f - b_{\text{det}} X_{fi} L_f \quad [29]$$

To compute the differentials, J must be computed from the known values of S and $X_f L_f$, as well as X_f , D , D_f , and L , which are given in Table 1. The computations are most efficiently carried out with the pseudo-analytical solution for biofilms of any thickness (Rittmann and McCarty, 1981), Equations 49–62 in Chapter 4.

Figure 7 summarizes the results for this example. Although absolute values are not comparable, the general trends are similar to those in the first 15 days in Figure 4, which is

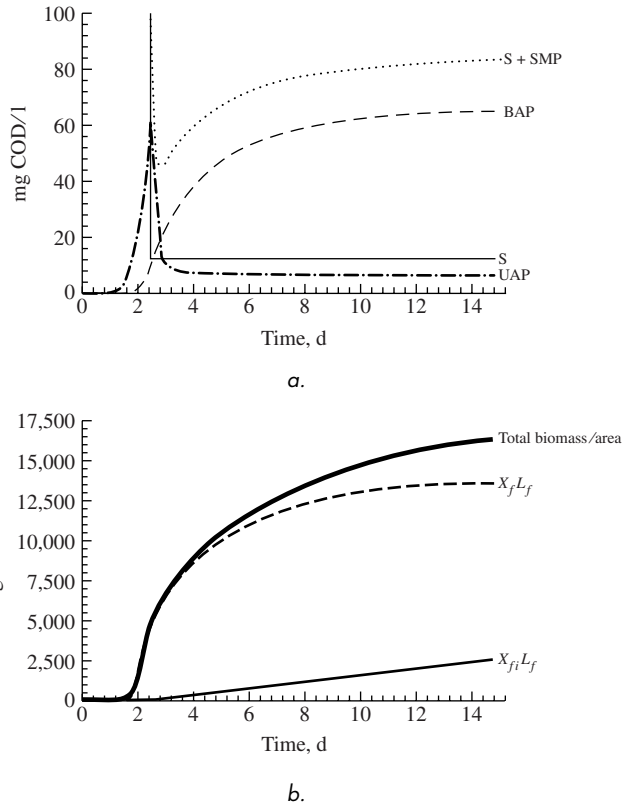


Figure 7 The gradual approach to steady state for a completely mixed biofilm reactor started from a small inoculum and fed continuously at $Q/hV = 1/d$ and $S^0 = 1,000 \text{ mg BOD}_L/l$. The biofilm is deep as it reaches steady state.

for a chemostat. First, rapid removal of substrate begins as the active biomass grows beyond the small inoculum. This leads to a steady-state value of S , which is followed by a gradual approach to steady state for active biomass ($X_f L_f$). Second, the soluble COD (SMP+S) has a “dip” as S declines rapidly, but before BAP formation is significant. Third, the effluent soluble COD is dominated by BAP as steady state is approached. Finally, active biomass is much greater than inert biomass for the conditions studied.

Figure 7 also shows some important differences, compared to Figure 4. The first difference is the change in slope for biomass growth at approximately 2 days. This change in biofilm growth rate indicates that the biofilm has become deep; hence, the flux and syntheses rates remain constant, but the loss rate continues to increase as $X_f L_f$ becomes larger. The second difference is that $X_f L_f$ and $X_{fi} L_f$ have not reached their steady states by 15 days. The reason for the continual slow growth of the biofilm is the expansion of the interior portions of the biofilm. The outer portion of the biofilm, which has net positive growth, is exporting active biomass to the interior portions, where it decays to form inert biomass.

Example 8

EFFECTS OF LOADING CHANGES ON A COMPLETELY MIXED BIOFILM REACTOR

A biofilm reactor is at an initial steady-state loading of

$$hV = 1,000 \text{ m}^3$$

$$Q = 5,000 \text{ m}^3/\text{d}$$

$$S^0 = 200 \text{ mg BOD}_L/\text{l}$$

$$aV = 200,000 \text{ m}^2$$

$$a/h = 200 \text{ m}^{-1}$$

$$b_{\text{det}} = 0.1/\text{d}$$

This gives a surface loading of 5 kg BOD_L/1,000 m²-day, which is approaching the high-load region, where the biofilm is deep. It is then subjected to a sudden step increase in S^0 to 400 mg/l. After the new steady state is achieved, the flow rate suddenly drops to $Q = 2,500 \text{ m}^3/\text{d}$, while S^0 remains at 400 mg/l. Equations 25 to 29 are the nonsteady-state mass balances.

The transient solution is shown in Figure 8. Because the biomass is retained by attachment and the liquid retention time is relatively short, S and UAP respond rapidly. UAP overshoots its new steady-state concentration during the time it takes the biomass accumulation to respond. S does not overshoot, and the overshooting for UAP is damped in this case, because the biofilm is deep, which means that its effectiveness factor increases as S rises quickly and decreases as S falls. BAP and $X_f L_f$ rise or fall gradually, while $X_{fi} L_f$ lags behind and does not reach a new steady state before the loads are changed.

The soluble effluent quality has a very interesting response in that SMP+S increases initially for both changes. In the former case, the sharp rise at first is due to the spike increase in S and UAP, while the long-term increase is due to BAP. For the latter change, the initial increase is caused by a sharp rise in BAP, which increases due to reduced advection loss when Q declines. As the biomass gradually declines in the latter case, BAP returns to near its level for the second period. The BAP response illustrates that advection is a major sink for BAP, which has relatively slow degradation kinetics.

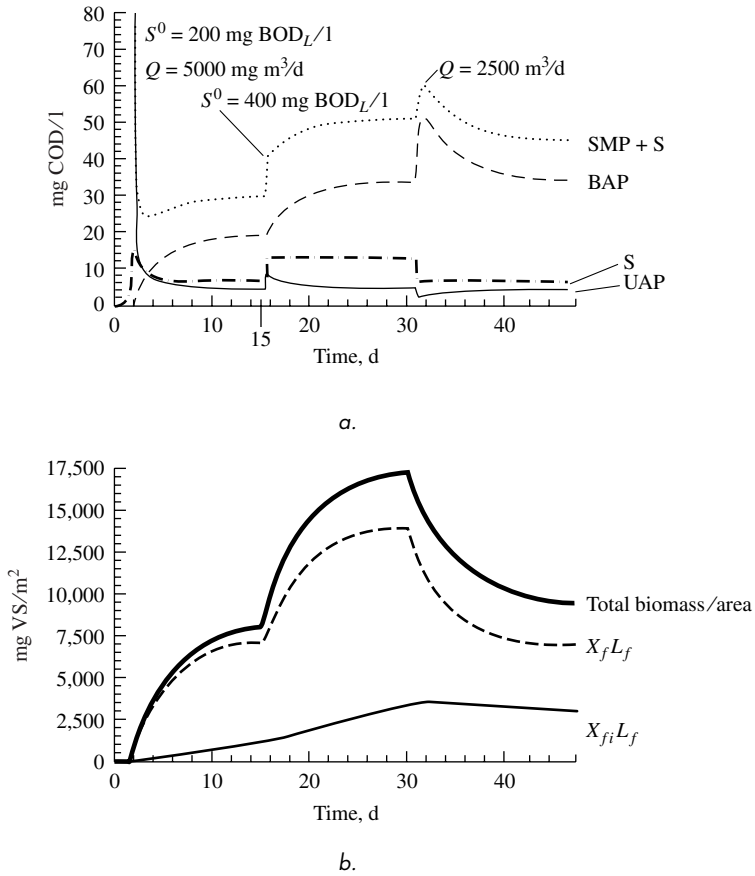


Figure 8 Response of a high-load, completely mixed biofilm reactor to changes in loading.

EFFECTS OF A LOADING CHANGE ON A LOW-LOAD BIOFILM REACTOR

Example 9

A low-loaded biofilm reactor has a nearly fully penetrated biofilm (recall Normalized Surface Loading in Chapter 4). The conditions giving a low loading are:

- $hV = 1,000 \text{ m}^3$
- $Q = 5,000 \text{ m}^3/\text{d}$
- $S^0 = 5 \text{ mg BOD}_L/\text{l}$
- $aV = 200,000 \text{ m}^2$
- $a/h = 200 \text{ m}^{-1}$
- $b_{\text{det}} = 0.1/\text{d}$

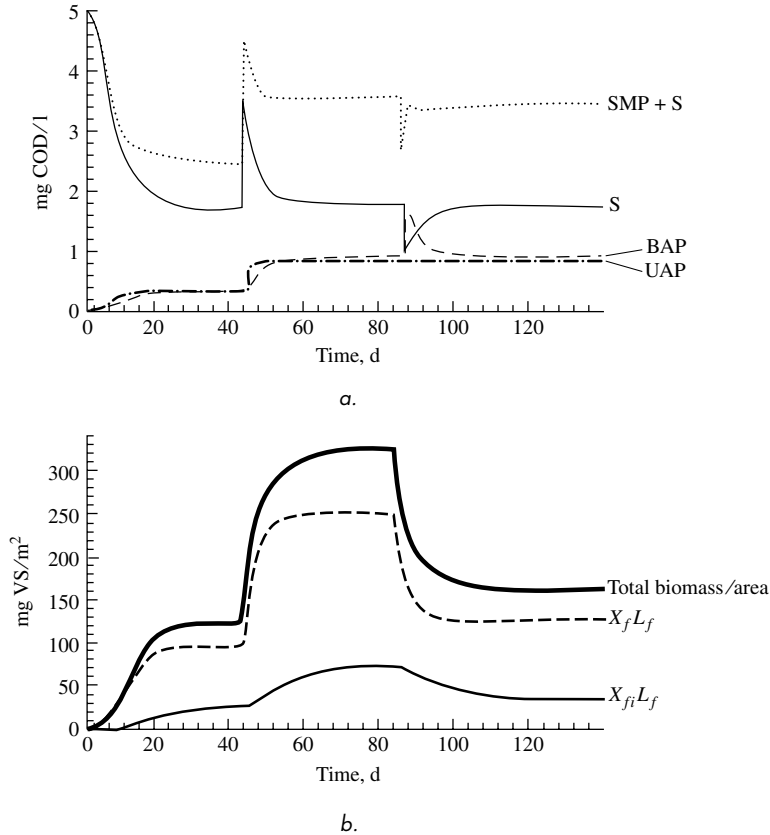


Figure 9 Response of a low-load, completely mixed biofilm reactor to changes in loading. An increase in S^0 to 10 mg BOD_L/l occurs at day 44, and a decrease in Q to 2,500 m³/d occurs at day 84.

These conditions give a surface loading of only 0.125 kg BOD_L/1,000 m²-d. The reactor first comes to steady state with this load. Then, it is subject to a sudden step increase in S^0 to 10 mg BOD_L/l at day 44. At day 84, the flow rate is decreased to 2,500 m³/d. Equations 25 to 29 again hold.

Figure 9 shows how the low-loaded biofilm responds. Compared to Figure 8, the overshooting for S is greater on a relative scale, since the fully penetrated biofilm cannot change its effectiveness factor in response to short-term changes in S . However, the long-term change in S is small, since the biofilm remains in the low-load region at steady state, and S stays near S_{\min} . Closely related is that S controls the response of the total soluble COD. Due to the low biofilm accumulation with the low-load biofilm, BAP is not the dominant soluble component, although it responds to the loading changes with the same trends as are seen in Figure 8. UAP is relatively more important in this case.

Although the biofilm responses are similar in Figures 8 and 9, the increase is slower, but proportionally greater for the low-load biofilm. The slower response comes about because the substrate concentration and flux are much lower for Figure 9. However, the increase in biofilm accumulation is greater at steady state, because the flux to low-load steady-state biofilms shows greater sensitivity to small changes in S .

EFFECTS OF A TEMPERATURE CHANGE ON A COMPLETELY MIXED BIOFILM REACTOR

Example 10

The biofilm reactor begins with the same starting conditions as in Example 8. A sudden 10°C temperature decrease at day 16 changes the kinetic parameters as follows:

\hat{q}	10 to 5	mg BOD _L /mg VS _{a-d}
\hat{q}_{UAP}	1.8 to 0.9	mg COD _P /mg VS _{a-d}
\hat{q}_{BAP}	0.1 to 0.05	mg COD _P /mg VS _{a-d}
b	0.15 to 0.075	d ⁻¹
k_2	0.09 to 0.045	mg COD _P /mg VS _{a-d}
D	1.0 to 0.78	cm ² /d
D_f	0.8 to 0.62	cm ² /d

The other parameters remain the same. Equations 25 to 29 remain appropriate.

Figure 10 shows the effects of the sudden temperature drop for the relatively high-load biofilm reactor. The short-term effects are modest. Although S and UAP increase about 20 to

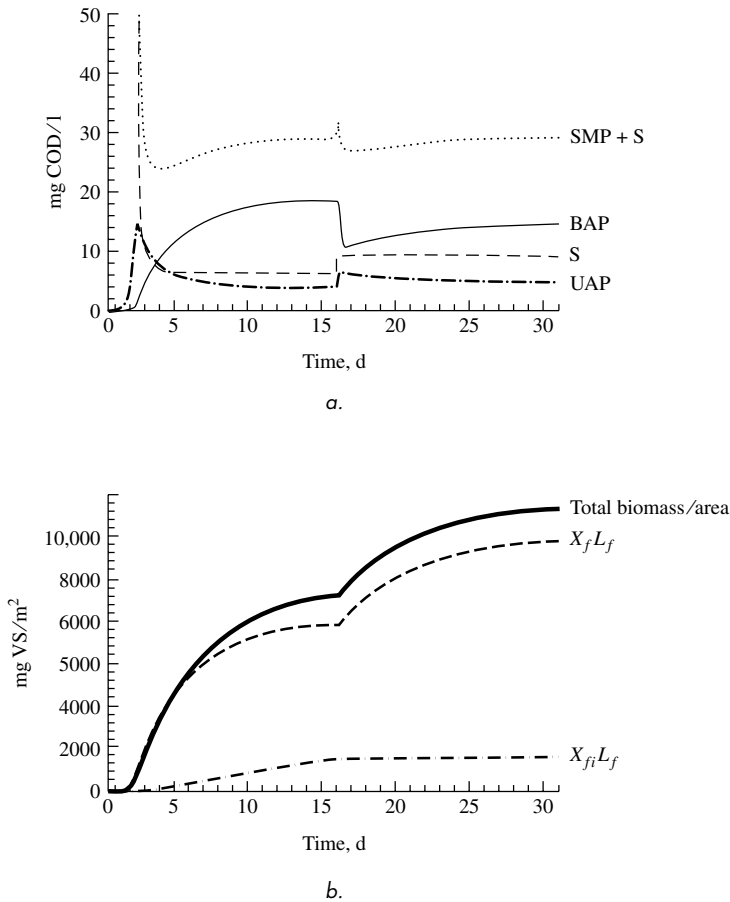


Figure 10 Effects of a sudden temperature drop (20°C to 10°C on day 16) on the performance of the completely mixed biofilm reactor.

50 percent, BAP declines about 40 percent. The net result is that the soluble COD (i.e., $S + \text{SMP}$) has a small oscillation and then is almost unchanged. S and UAP increase because their degradation rates decline. BAP decreases because its production rate declines, but its main sink, advection is unchanged.

In the long term, the active biomass increases, since the rising substrate concentration keeps the flux relatively constant, while the decay rate slows. Detachment becomes a more important loss mechanism, which makes the inert biomass a smaller proportion of the total biofilm accumulation.

MULTISPECIES SYSTEMS

The microbial communities that develop in treatment processes, as well as in nature, are comprised of many different species and strains. For engineering design and operation, we often choose to ignore the diversity when the different microorganisms are performing essentially the same metabolic functions. For instance, we often have no need to distinguish among the several strains of aerobic heterotrophs that oxidize BOD in parallel. Instead, we treat the biomass as though it were a single species. This simplified approach, which is the basis for Chapters 3, 4, and 5 and this material up to here, works well when the distinctions among the different strains are minor. Then, all major trends in process performance are identified without introducing unnecessary complications.

Environmental biotechnology also has many situations in which the distinctions among the different strains and species are dramatic and of the utmost importance. Table 2 lists several important systems in which different bacterial types coexist in multispecies communities. In some cases, several interactions occur together. In these cases, our representation of these systems requires a *multispecies* approach, in which different microorganism types and their unique metabolic reactions must be described individually. The remainder of this material presents the techniques needed to describe multispecies systems through quantitative modeling. Through multispecies modeling, we can begin to explore how microbial ecology affects process performance.

At its simplest, multispecies modeling involves writing the usual mass-balance equations, but for several types of active biomass and their rate-limiting substrates. So, instead of having one X_a to represent active biomass, it is subdivided into X_{a1} , X_{a2} , \dots , X_{an} , in which the second subscript identifies a particular type of microorganism. Likewise, mass balances are needed for S_1, S_2, \dots, S_n which are the corresponding rate-limiting substrates. Clearly, the number of equations to be solved increases as unique species are added.

Multispecies modeling can be substantially more involved than is suggested solely by the addition of extra mass balances. Complexity is created by the interactions that frequently occur among the different microorganism types. These interactions include: two or more species competing for the same substrate, one species generating a product that is the substrate for another species, one species using as its substrate

Table 2 Examples of Multispecies Communities Important in Environmental Biotechnology

Microbial Groups	Interactions	Example Applications
1. Aerobic heterotrophs + autotrophic nitrifiers	<ul style="list-style-type: none"> • Competition for O₂ (ea) • Competition for NH₄⁺ (ea and n) • Product (NO₂⁻) can be substrate (ed) 	<ul style="list-style-type: none"> • Aerobic treatment of wastewater and drinking water • Rivers and lakes
2. Facultative heterotrophs + autotrophic nitrifiers	<ul style="list-style-type: none"> • Competition for O₂ (ea) • Competition for NH₄⁺ (ed and n) • Competition for NO₃⁻ (ea and n) • Products (NO₂⁻ and NO₃⁻) can be substrates (ea) • Product (NO₂⁻) can be substrate (ed) 	<ul style="list-style-type: none"> • Nutrient removal in wastewater treatment • Groundwater • Sediments
3. Filamentous versus floc-forming aerobic heterotrophs	<ul style="list-style-type: none"> • Competition for organic (ed) and O₂ (ea) 	<ul style="list-style-type: none"> • Activated sludge
4. Methanogens and sulfate-reducing bacteria (SRB)	<ul style="list-style-type: none"> • Competition for acetate and H₂ (ed) • Fermentation product of SRB can be substrate for methanogens 	<ul style="list-style-type: none"> • Anaerobic wastewater and sludge treatment • Sediments • Groundwater
5. Aerobic heterotrophs, methanogens, SRB, Fe ³⁺ -reducing bacteria, S ²⁻ -oxidizing bacteria (SOB)	<ul style="list-style-type: none"> • Competition for acetate and H₂ (ed) • Fermentation product of SRB can be substrate for methanogens and Fe³⁺-reducing bacteria • Product of SRB is substrate (ed) for SOB • Competition for O₂ (ea) by aerobic heterotrophs and SOB 	<ul style="list-style-type: none"> • Sediments • Groundwater • Microbial mats

NOTES: 1. ea = electron-acceptor substrate; ed = electron-donor substrate; n = nutrient.
 2. All systems have competition for space in aggregates.

a material that is a nutrient for another species, and different species competing for space within aggregates.

This material uses the first system in Table 2— aerobic heterotrophs plus autotrophic nitrifiers—to develop the modeling approach and demonstrate the key trends. This system exhibits all of the interactions of interest and occurs widely in treatment technology and nature. It is also of great interest because the two microbial groups are physiologically very different, which means that they absolutely must not be treated as one “biomass.” We begin with the most basic components and interactions. Then, components and interactions are added to reflect the system more accurately, to show how they are implemented, and to see their effects.

BASIC MULTISPECIES MODEL

In its simplest form, the model multispecies system is comprised of two active species: aerobic heterotrophs and autotrophic nitrifiers. For the basic model, we consider two types of active biomass: heterotrophs at concentration X_{ah} , and nitrifiers at concentration X_{an} . Each has a separate rate-limiting electron-donor substrate: BOD at concentration S and NH₄⁺-N at concentration N_1 . Each species uses O₂ as the electron acceptor, but we assume the O₂ is not limiting for the basic model. NH₄⁺-N

also is used by the heterotrophs as a nutrient, and we include that aspect in the basic model. We also ignore soluble microbial products in the basic model. For this simplest multispecies model, we do not divide the nitrifiers into ammonium and nitrite oxidizer; instead, we assume that ammonium is oxidized completely to nitrate.

Table 3 lists the kinetic and stoichiometric parameters for this system. Not all are needed for the basic model, but all will be explained as they are added later. A key distinction between the heterotrophs and nitrifiers is θ_X^{\min} : The limiting values of θ_X^{\min} are 0.25 and 1.1 days, respectively, for the heterotrophs and nitrifiers. Thus, the heterotrophs are much faster growers. The S_{\min} values for the two microbial types are 0.74 mg BOD_L/l and 0.055 mg NH₄⁺-N/l; thus steady-state concentrations on both substrates can be driven to low values.

Nonsteady-state mass balances are written for both substrates, both biomass types, and inert biomass. For a chemostat, they are:

$$V \frac{dS}{dt} = QS^0 - QS - \frac{\hat{q}_h S}{K_h + S} X_{ah} V \quad [30]$$

$$V \frac{dN_1}{dt} = QN_1^0 - QN_1 - \frac{\hat{q}_{n1} N_1}{K_{n1} + N_1} X_{an} V + \gamma_N f_d b_n X_{an} V \quad [31]$$

$$- \gamma_N \left[Y_h \frac{\hat{q}_h S}{K_h + S} - f_d b_h \right] X_{ah} V$$

Table 3 Kinetic and Stoichiometric Parameters Used for the Multispecies System (Including Aerobic Heterotrophs and Nitrifiers)

Parameter	Heterotrophs	Nitrifiers
\hat{q}	10 mg BOD _L /mg VSS _{ah} -d	2.3 mg NH ₄ ⁺ -N/mg VSS _{an} -d
K	20 mg BOD _L /l	1.0 mg NH ₄ ⁺ -N/l
K_0	0.1 mg O ₂ /l	0.5 mg O ₂ /l
\hat{q}_{UAP}	1.8 mg COD _p /mg VSS _{ah} -d	n.a.
K_{UAP}	100 mg COD _p /l	n.a.
\hat{q}_{BAP}	0.1 mg COD _p /mg VSS _{ah} -d	n.a.
K_{BAP}	85 mg COD _p /l	n.a.
k_1	0.12 mg COD _p /mg BOD _L	0.11 mg COD _p /mg NH ₄ ⁺ -N
k_2	0.09 mg COD _p /VSS _{ah} -d	0.09 mg COD _p /mg VSS _{an} -d
b	0.15/d	0.05/d
f_d	0.8	0.8
Y	0.42 mg VSS _{ah} /mg BOD _L	0.41 mg VSS _{an} /mg NH ₄ ⁺ -N
γ_N	0.124 mg N/mg VSS _{ah}	0.124 mg N/mg VSS _{an}

n.a. = not applicable.

$$V \frac{dX_{ah}}{dt} = QX_{ah}^0 - QX_{ah} + \left[Y_h \frac{\hat{q}_h S}{K_h + S} - b_h \right] X_{ah} V \quad [32]$$

$$V \frac{dX_{an}}{dt} = QX_{an}^0 - QX_{an} + \left[Y_n \frac{\hat{q}_{n1} N_1}{K_{n1} + N_1} - b_n \right] X_{an} V \quad [33]$$

$$V \frac{dX_i^0}{dt} = QX_i^0 - QX_i + (1 - f_d) [b_h X_{ah} + b_n X_{an}] V \quad [34]$$

Key interactions are represented in Equation 31. The third term on the right side is the uptake of NH_4^+ -N by oxidation and synthesis of new nitrifying biomass. The fourth term is the release of NH_4^+ -N from endogenous respiration of nitrifiers. The fifth term is the *net uptake* of NH_4^+ -N for heterotroph synthesis. Thus, both groups of microorganisms are consuming and releasing NH_4^+ -N. γ_N is the ratio of N to VS in biomass, 0.124 mg N/mg VS for $\text{C}_5\text{H}_7\text{O}_2\text{N}$.

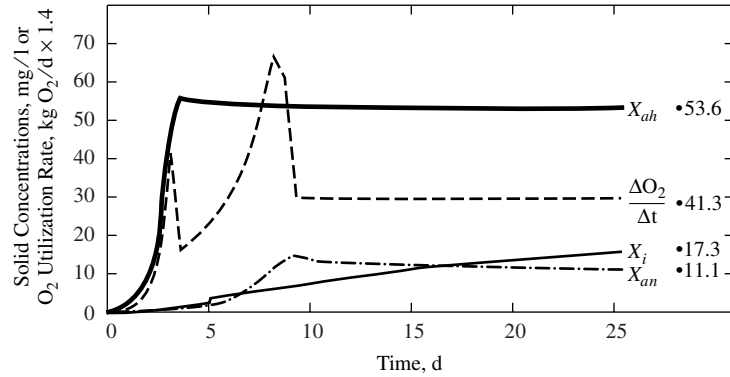
Figure 11 shows how this system approaches steady state from a small inoculum (1 mg VS_a /l each of heterotrophs and nitrifiers) when the reactor conditions are:

$$\begin{aligned} V &= 1,000 \text{ m}^3 \\ Q &= 100 \text{ m}^3/\text{d} \\ S^0 &= 300 \text{ mg BOD}_L/\text{l} \\ N_1^0 &= 50 \text{ mg NH}_4^+\text{-N/l} \\ X_{ah}^0 &= X_{an}^0 = X_i^0 = 0 \\ N_1^{\text{in}} &= 20 \text{ mg NH}_4^+\text{-N/l} \\ S^{\text{in}} &= 300 \text{ mg BOD}_L/\text{l} \end{aligned}$$

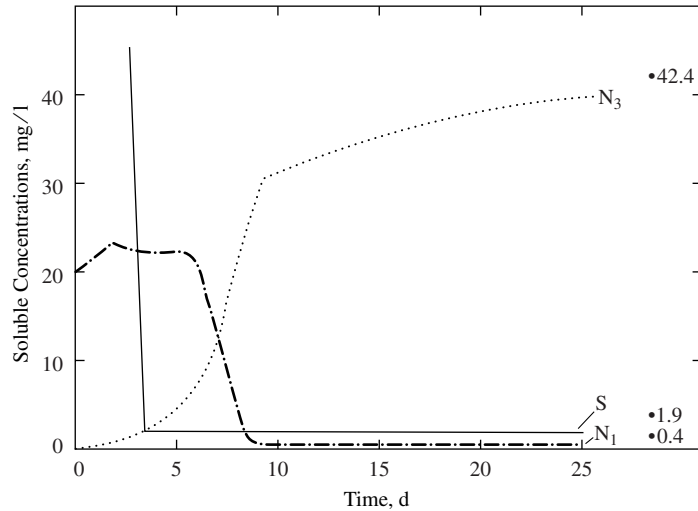
As usual, the concentrations were updated by marching forward and using the differential values in Equations 30 to 34. Because of their faster specific growth rate, the heterotrophs reach their steady-state concentration much sooner than do the nitrifiers. Likewise, S reaches its final steady-state value sooner than N_1 . NH_4^+ -N experiences two periods of declining concentration. In the first 5 days, it declines due to synthesis of the heterotrophs. Later, nitrification becomes the major sink and drives N_1 to its final, very low concentration. Because it “grows” much slower than the active forms of biomass, the inert biomass is not at steady state in 25 days, even though the active forms are essentially at steady state.

ADDING THE CONSUMPTION OF THE ELECTRON ACCEPTORS

The rate of consumption of O_2 , the electron acceptor, is of great importance. It is computed most directly by combining the rates used in the basic model with stoichiometry. Expressed in mass per time units, the rate of oxygen consumption, denoted



a.



b.

Figure 11 Approach to steady state for a chemostat with $S^0 = 300$ mg/l, $N_1^0 = 50$ mg/l, $\theta = 10$ d, and for the simplest multispecies model. The symbols and numbers at the far right are the ultimate steady-state values. The values at $t = 0$ d use the initial conditions, which are not the same as the input values. The value for $\Delta O_2/\Delta t$ is 1.4 times the value shown on the vertical scale.

$V[-\frac{dO_2}{dt}]$, is

$$V \left[-\frac{dO_2}{dt} \right] = \alpha_h \frac{\hat{q}_h S}{K_h + S} X_{ah} V + \alpha_n \frac{\hat{q}_{n1} N_1}{K_{n1} + N_1} X_{an} V + 1.42 f_d b_h X_{ah} V + 1.42 f_d b_n X_{an} V$$

[35]

The first two terms are the direct oxygen consumption for substrate oxidations. The

α_h and α_n values are proportional to the respective f_e^0 values for heterotrophs and ammonium oxidizers. For this basic model,

$$\alpha_h = 1 - f_{sh}^0 = 1 - 1.42 \frac{\text{mg O}_2}{\text{mg VSS}_{ah}} Y_h = (1 - 1.42 \times 0.42) = 0.4 \text{ mg O}_2/\text{mg BOD}_L$$

$$\alpha_n = 4.57 \frac{\text{mg O}_2}{\text{mg NH}_4^+-\text{N}} - 1.42 \frac{\text{mg O}_2}{\text{mg VSS}_{an}} \times 0.41 \frac{\text{mg VSS}_{an}}{\text{mg NH}_4^+-\text{N}}$$

$$- 4.57 \frac{\text{mg O}_2}{\text{mg NH}_4^+-\text{N}} \times 0.124 \frac{\text{mg NH}_4^+-\text{N}}{\text{mg VSS}_{an}} \times 0.41 \frac{\text{mg VSS}_{an}}{\text{mg NH}_4^+-\text{N}}$$

$$= 3.76 \text{ mg O}_2/\text{mg NH}_4^+-\text{N}$$

For computing α_n , the first term is the total removal of NH_4^+-N , expressed as O_2 demand. The second term is the O_2 demand invested as C in synthesis, and the third term is the O_2 demand invested as N in synthesis.

The third and fourth terms on the right side of Equation 35 are the consumptions of O_2 due to endogenous respiration of the heterotrophic and nitrifying biomasses, respectively.

Figure 11 also plots the time course for O_2 demand for the approach to steady state. Oxygen consumption develops in two stages, the first corresponding to the growth of the heterotrophs and the second corresponding to the growth of the nitrifiers. In both cases, a strong pulse of O_2 demand builds and subsides due to utilization of substrate stored in the reactor volume. At steady state, approximately 78 percent of the influent total oxygen demand ($= 300 + 4.57 \cdot 50 = 529 \text{ mg O}_2/\text{l}$) is being consumed by oxygen respiration. Most of the remaining oxygen demand exits as biomass ($1.42 \cdot (X_{ah} + X_{an} + X_i) = 115 \text{ mg O}_2/\text{l}$ at steady state).

PRODUCTION OF NO_3^--N

The production of NO_3^--N is proportional to f_e for the nitrifiers. The NO_3^--N concentration, called N_3 , is added to the model by using Equation 36:

$$V \frac{dN_3}{dt} = QN_3^0 - QN_3 + (1 - \gamma_n Y_n) \frac{\hat{q}_{n1} N_1}{K_{n1} + N_1} X_{an} V \quad [36]$$

in which $\gamma_n Y_n$ is the fraction of NH_4^+-N synthesized into ammonium-oxidizer biomass N , instead of being oxidized to NO_3^- .

Figure 11 also shows the gradual build-up of NO_3^--N as nitrification becomes established. At steady state, 84 percent of the input NH_4^+-N exists as NO_3^- , while 16 percent leaves in the biomass plus NH_4^+-N . The NO_3^--N concentration continues to build up once full nitrification is in effect. This is caused by the large reactor detention time (10 d), which gives a washout period of about 3θ , or 30 days.

PRODUCTION AND CONSUMPTION OF SMP

The production and consumption of UAP and BAP affect the flow of electrons, the accumulation of nitrifiers versus heterotrophs, and the effluent quality. UAP and BAP contain O_2 demand that is diverted from biomass accumulation and the consumption of oxygen. Coming from biomass, BAP also contains nitrogen that is neither nitrified

nor contained in biomass. Furthermore, autotrophic synthesis of nitrifier biomass transfers electrons from an inorganic reservoir ($\text{NH}_4^+ - \text{N}$) to organic reservoirs (nitrifier biomass and BAP).

The mass-balance equations that take into account UAP, BAP, and their effects on the flows of electrons and nitrogen are given below. Only the mass-balance equations for original substrate, $\text{NO}_3^- - \text{N}$, and inert biomass are unchanged:

$$V \frac{dS}{dt} = QS^0 - QS - \frac{\hat{q}_h S}{K_h + S} X_{ah} V \quad [37]$$

$$V \frac{dN_1}{dt} = QN_1^0 - QN_1 - \frac{\hat{q}_{n1} N_1}{K_{n1} + N_1} X_{an} + \gamma_N f_d b_n X_{an} V - \gamma_N \left[Y_h \frac{\hat{q}_h S}{K_h + S} + Y_h \frac{\hat{q}_{\text{UAP}} \text{UAP}}{K_{\text{UAP}} + \text{UAP}} + \left(Y_h - \frac{1}{1.42} \right) \frac{\hat{q}_{\text{BAP}} \text{BAP}}{K_{\text{BAP}} + \text{BAP}} - f_d b_h \right] X_{ah} V \quad [38]$$

$$V \frac{dX_{ah}}{dt} = QX_{ah}^0 - QX_{ah} + \left[Y_h \left(\frac{\hat{q}_h S}{K_h + S} + \frac{\hat{q}_{\text{UAP}} \text{UAP}}{K_{\text{UAP}} + \text{UAP}} + \frac{\hat{q}_{\text{BAP}} \text{BAP}}{K_{\text{BAP}} + \text{BAP}} \right) - b_h - \frac{k_{2h}}{1.42} \right] X_{ah} V \quad [39]$$

$$V \frac{dX_{an}}{dt} = QX_{an}^0 - QX_{an} + \left[Y_n \frac{\hat{q}_{n1} N_1}{K_{n1} + N_1} - b_n - \frac{k_{2n}}{1.42} \right] X_{an} V \quad [40]$$

$$V \frac{dX_i}{dt} = QX_i^0 - QX_i + (1 - f_d)[b_n X_{an} + b_h X_{ah}]V \quad [41]$$

$$V \frac{d\text{UAP}}{dt} = -Q\text{UAP} + k_{1h} \frac{\hat{q}_h S}{K + S} X_{ah} V + k_{1n} \frac{\hat{q}_{n1} N_1}{K_{n1} + N_1} X_{an} V - \frac{\hat{q}_{\text{UAP}} \text{UAP}}{K_{\text{UAP}} + \text{UAP}} X_{ah} V \quad [42]$$

$$V \frac{d\text{BAP}}{dt} = -Q\text{BAP} + k_{2h} X_{ah} V + k_{2n} X_{an} V - \frac{\hat{q}_{\text{BAP}} \text{BAP}}{K_{\text{BAP}} + \text{BAP}} X_{ah} V \quad [43]$$

$$V \frac{dN_3}{dt} = QN_3^0 - QN_3 + (1 - \gamma_n Y_n) \frac{\hat{q}_{n1} N_1}{K_{n1} + N_1} X_{an} V \quad [44]$$

$$V \left[\frac{d\text{O}_2}{dt} \right] = \alpha_h \frac{\hat{q}_h S}{K_h + S} X_{ah} V + \alpha_{hP} \left[\frac{\hat{q}_{\text{UAP}} \text{UAP}}{K_{\text{UAP}} + \text{UAP}} + \frac{\hat{q}_{\text{BAP}} \text{BAP}}{K_{\text{BAP}} + \text{BAP}} \right] X_{ah} V + \alpha_n \frac{\hat{q}_{n1} N_1}{K_{n1} + N_1} X_{an} V + 1.42 f_d (b_h X_{ah} + b_n X_{an}) V \quad [45]$$

in which

$$\alpha_h = (1 - 1.42Y_h - k_{1h}) = (1 - 1.42 \cdot 0.42 - 0.2) = 0.2 \text{ mg O}_2/\text{mg BOD}_L$$

$$\alpha_{hP} = (1 - 1.42Y_h) = (1 - 1.42 \cdot 0.42) = 0.4 \text{ mg O}_2/\text{mg BOD}_L$$

$$\alpha_n = (4.57 - 1.42Y_n - 4.57\gamma_N Y_n - k_{1n})$$

$$= (4.57 - 1.42 \cdot 0.41 - 4.57 \cdot 0.124 \cdot 0.41 - 0.11) = 3.65 \text{ mg O}_2/\text{mg NH}_4^+\text{-N.}$$

Figure 12 shows the time course of the variables for the same conditions as used before. Comparing Figure 12 with Figure 11 shows that the major trends remain similar. However, consideration of SMP slightly slows the growth of heterotrophic biomass at first. In the long term, heterotrophic utilization of SMP produced by themselves and by the nitrifiers (after about 10 days) counteracts much of the impact of SMP generation by the heterotrophs. The nitrifier biomass (X_{an}) grows more slowly, and it declines somewhat due to the loss of BAP, which it cannot utilize. The latter effect causes N_1 to be a bit higher in Figure 12. The effluent soluble organic material is dominated by SMP, particularly BAP.

Oxygen consumption (not shown) accounts for 72 percent of the influent oxygen demand at steady state. This is reduced from the prior example, because SMP now

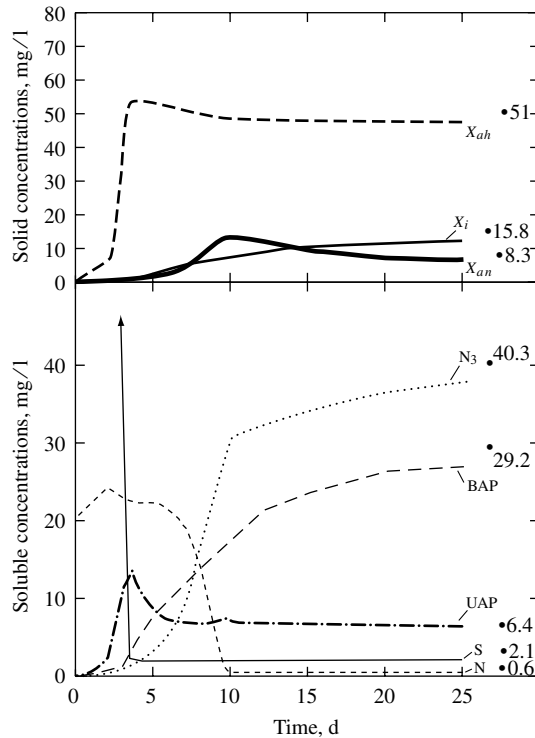


Figure 12 Approach to steady state from a small inoculum when SMP are considered.

carries away 7 percent of the oxygen demand. The biomass also contains less oxygen demand, 106 mg/l. The BAP contains N , and this means that less N ends up in effluent NO_3^- -N, compared to Figure 11.

SEQUENCING BATCH REACTOR

Sequencing batch reactors, formerly called fill-and-draw systems, are a hybrid of continuous-feed and batch operation. The influent is applied cyclically and alternates with periods of reaction, quiescent settling, and effluent withdrawal. For this example, a 4-h cycle is used:

aerated fill	60 min
aerated react	150 min
settling and effluent withdrawal	20 min
effluent withdrawal	10 min

The system parameters are:

$$V = \text{Maximum volume} = 1,000 \text{ m}^3$$

$$\text{Volume added each cycle: } 160 \text{ m}^3$$

$$Q = \text{Average flow rate} = 960 \text{ m}^3/\text{d}$$

$$S^0 = 500 \text{ mg BOD}_L/\text{l}$$

$$N_1^0 = 50 \text{ mg NH}_4^+\text{-N/l}$$

$$X_a^0 = X_i^0 = 0$$

$$\theta_X = 10 \text{ d}$$

It is assumed that no reactions occur during the unaerated periods. The instantaneous flow rates are $4Q$ and $24Q$ during the fill and withdrawal periods, where Q is the average flow rate. The flow rate is zero for react periods. All sludge withdrawal for θ_X control occurs in the last 10 min of the quiescent period. The average mass per time sludge withdrawal rate is XV/θ_X , although sludge wasting occurs at a much faster rate during its removal period. The instantaneous sludge-withdrawal rate for use in the differential rate expression is $(24/V)(XV/\theta_X) = 24X/\theta_X$.

Nonsteady-state mass balances are needed for S , X_{ah} , X_{an} , X_i , UAP, BAP, N_1 , and N_3 . In addition, the volume changes, which requires a mass balance on water. Therefore, each mass balance (i.e., Equations 37 to 45) includes a term of the form $-X \cdot dV/dt$ on the right side to account for the dilution or concentration of materials that are not carried in or out of the reactor in the influent or effluent.

The set of mass balance equations was solved by the usual marching-forward technique until all variables stabilized to the same values for the same time in every cycle. Figure 13 presents the variation in concentrations across one cycle. The biggest changes occur for S , which increases rapidly during the fill period, but is degraded to zero concentration well before the end of the react period. Like substrate BOD_L ,

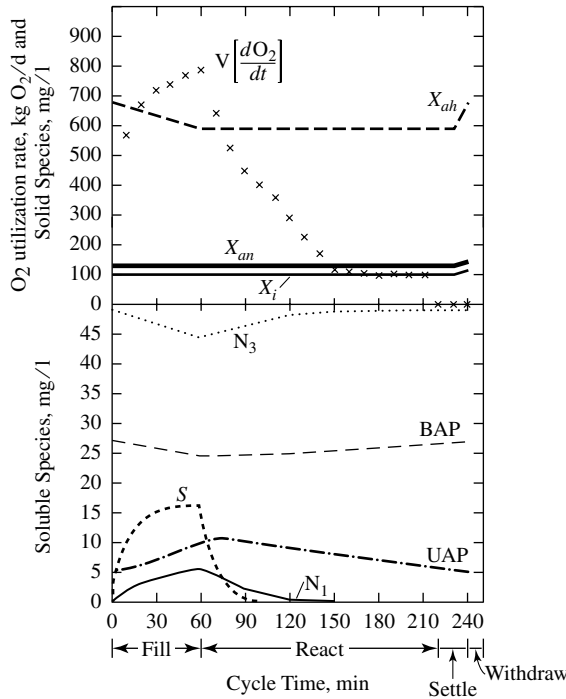


Figure 13 Changes in S , BAP , UAP , NH_4^+ - N (N), NO_3^- - N , (N_3), inert biomass (X_i), active heterotrophs (X_{ah}), active nitrifiers (X_{an}), and oxygen utilization rate ($V[dO_2/dt]$) through a 240-min cycle of the SBR.

NH_4^+ - N increases during the fill and becomes very small during react. UAP , which is generated in proportion to S and N utilization, shows a steady rise during the fill period. X_{ah} , X_{an} , X_i , and BAP show relatively small changes during the cycle. This situation is created by the ratio θ_X/θ being substantially greater than unity. All solids concentrations rise significantly during effluent withdrawal, since solids-free water is removed, and the remaining volume contains all the solids from the end of the cycle. N_3 (NO_3^- - N) also is relatively constant, since nitrification is essentially 100 percent in this example.

MULTISPECIES BIOFILMS

In addition to all of the interactions that occur for multispecies suspended-growth systems, multispecies biofilms have the added possibility of stable spatial organizations. In short, different locations in the biofilm serve as unique *niches* for certain types of microorganisms to thrive. Thus, a complex microbial ecology can arise in

which specialized microbial types or reactions occur in zones or clusters within the biofilm. Spatial zoning in biofilms is accentuated because the physical structure of biofilms can remain intact over extended time spans. Hence, long-term stability of niches provides a strong ecological selection by location in the biofilm.

The fundamental driving force for spatial organization is a strong concentration gradient inside the biofilm. Concentration gradients occur when intense reaction rates coincide with limited mass transfer rates. Because substrate supply to biofilms normally is restricted to the surface area exposed to the bulk liquid, while internal mass transfer is via diffusion, the mass-transfer rates are inherently limited. Locally high biomass density within a biofilm gives the potential for highly intense reaction rates.

A second fundamental driving force for spatial organization is that certain biomass-loss mechanisms are focused at the outer surface. Detachment by erosion and predation occur mainly at the biofilm's outer surface, while inner portions are protected from their direct effects.

The confluence of these two driving forces creates a generalized selection:

- The *outer surface* selects for microorganisms that can grow rapidly in the presence of a high concentration of their substrate; the high growth rate allows them to overcome the higher loss rates.
- The *inner surface* selects for microorganisms that are slow growers and benefit most from being protected from losses.

Extensive modeling results (Rittmann and Manem, 1992; Wanner and Gujer, 1986; Kissel, McCarty, and Street, 1984; Furumai and Rittmann, 1994; Rittmann, Schwarz, and Sáez, 2000) and limited experimental measurements (Rittmann and Manem, 1992; Rittmann, Trinet, Amar, and Chang, 1992; Watanabe, Okabe, Hirata, and Masuda, 1995) support the generalized selection criteria. Figure 14 (from Rittmann and Manem (1992)) shows the model-predicted distribution according to biomass type for a steady-state multispecies biofilm. The fastest growers, the heterotrophs, dominate the outer surface when their substrate (acetate) is present at a nontrivial concentration. The “slowest grower” is the inert biomass, which always accumulates most near the attachment surface, where it gains the greatest protection from detachment. The autotrophic nitrifiers tend to accumulate behind the heterotrophs, when heterotrophs are significant. This arrangement gives them added protection from detachment, which is more valuable to them than the increase in mass-transport distance for their substrate, $\text{NH}_4^+\text{-N}$. Thus, an increase in the acetate concentration in the bulk liquid causes the total thickness of the biofilm to increase, allows the slower growing nitrifiers and inerts to exist farther from the outer surface, and thereby greatly increases the accumulation of inerts.

Figure 15, also from Rittmann and Manem (1992), shows that the model predictions and experimental measurements agree that increasing the surface loading and, therefore, bulk concentration of acetate caused the bulk concentration of ammonium to increase. For these experiments, a completely mixed biofilm reactor came to steady state with different acetate loadings, but a constant $\text{NH}_4^+\text{-N}$ loading. The increase

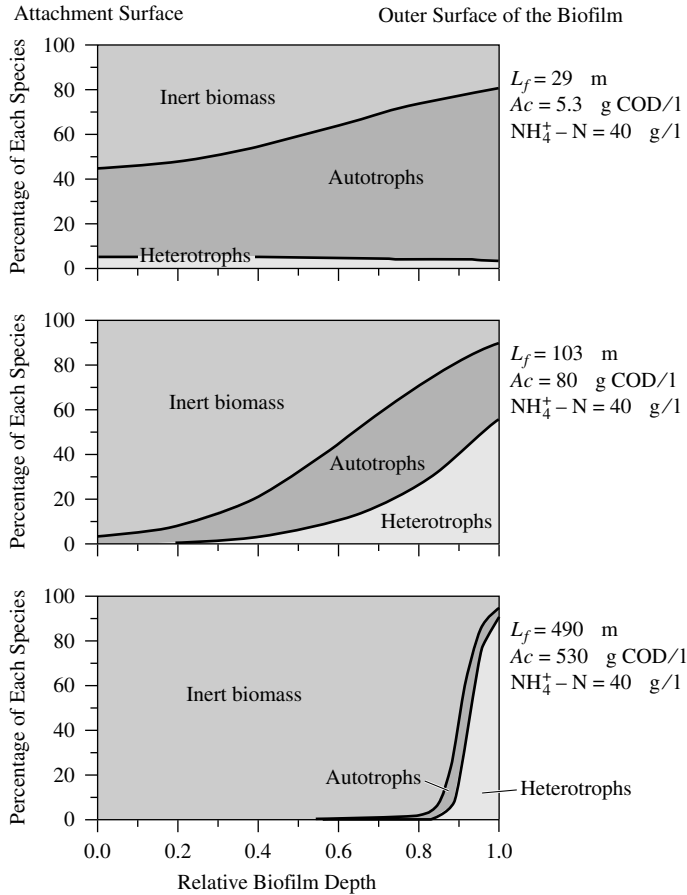


Figure 14 Model-predicted distributions of heterotroph, nitrifier, and inert biomasses in a multispecies steady-state biofilm exposed to an $\text{NH}_4^+ - \text{N}$ concentration of $40 \mu\text{g/l}$ and varying acetate concentrations.

bulk-liquid concentration of $\text{NH}_4^+ - \text{N}$ was caused by the nitrifiers being farther from the biofilm’s outer surface.

Although the surface loss rates act most directly on the species at the outer surface, the long-term effects alter the slowest growing species. For example, an increase to the detachment rate ultimately decreases the accumulation of inert biomass more dramatically than it decreases the accumulation of the fast-growing heterotrophs (Manem, 1988). Figure 16 shows how a steady-state biofilm that is dominated by inert biomass and nitrifiers for very low detachment sequentially loses the inerts and then the nitrifiers as the detachment-rate coefficient increases and biofilm thickness decreases.

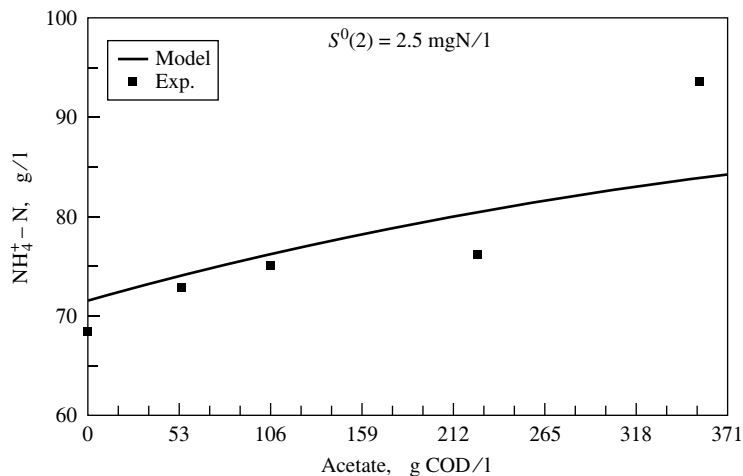


Figure 15 An increase in the acetate concentrations in the bulk liquid causes the bulk $\text{NH}_4^+\text{-N}$ concentration to rise, even though the $\text{NH}_4^+\text{-N}$ loading to the completely mixed biofilm reactor was unchanged.

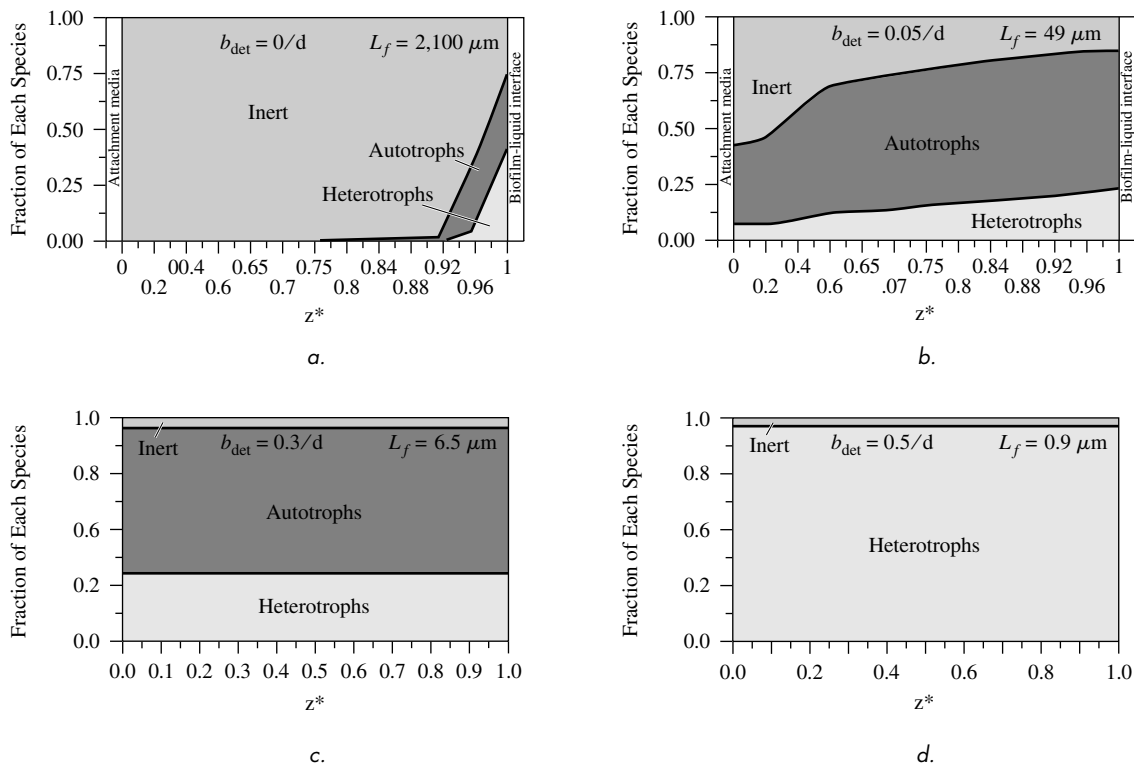


Figure 16 The progression from a multispecies steady-state biofilm to one of only heterotrophs as the detachment rate increases. The bulk concentrations of acetate and $\text{NH}_4^+\text{-N}$ are 53 and 100 $\mu\text{g/l}$, respectively.

MODELING MULTISPECIES BIOFILMS

Mathematical modeling of a multispecies biofilm involves merging the methods of Chapter 4 with the multispecies considerations of this topic. For the soluble species, such as substrates and products, the various rate expressions presented earlier are applied to a differential section, or slice, of biofilm. The second-order reaction-with-diffusion format is maintained. For the biomass species, multispecies modeling involves keeping track of each biomass type, as well as accounting for the movement of biomass from one section to another due to the net growth or loss of the biofilms.

Soluble Species The mass balance on NH_4^+ -N for a differential section of biofilm illustrates how the mass balance is set up for a soluble substrate. In this example, the multispecies biofilm contains aerobic heterotrophs, nitrifiers, and inert biomass. It is assumed that the densities of each biomass type are known as a model input or as a model-computed output. In parallel with the modeling used here for a chemostat, the heterotrophs utilize original substrate (S), UAP, and BAP; they form UAP, BAP, and new heterotrophic biomass; the nitrifiers oxidize NH_4^+ -N to NO_3^- -N, generate UAP and BAP, but do not consume UAP or BAP; and both biomass types decay through endogenous respiration and formation of inert biomass (X_i).

Soluble species quickly reach steady state at any position in the biofilm (Kissel et al., 1984; Wanner and Gujer, 1986). Thus, the steady-state mass-balance equation for NH_4^+ -N (N_1) is:

$$0 = D_{fn1} \frac{d^2 N_1}{dz^2} - \frac{\hat{q}_{n1} N_1}{K_n + N_1} X_{an} + \gamma_n f_d b_n X_{an} - \gamma_n \left[Y_h \frac{\hat{q}_S}{K_h + S} + Y_h \frac{\hat{q}_{\text{UAP}} \text{UAP}}{K_{\text{UAP}} + \text{UAP}} - f_d b_h + \left(Y_h - \frac{1}{1.42} \right) \frac{\hat{q}_{\text{BAP}} \text{BAP}}{K_{\text{BAP}} + \text{BAP}} \right] X_{ah} \quad [46]$$

in which all variables have values specific for the biofilm section being addressed. The solution for $N_1(z)$ makes this mass-balance equation true for all z . The resemblance between the right-hand sides of Equation 46 and Equation 38 is clear. Instead of advective transport, as in a chemostat, the biofilm has diffusive transport, which depends on the substrate concentrations in adjacent biofilm sections. Once the concentration profiles are known, the fluxes into or out of the biofilm can be computed from Fick's first law at the outer surface, e.g.,

$$J_{N1} = -D_{fn1} \left. \frac{dN_1}{dz} \right|_{z=0} \quad [47]$$

Equation 46 shows the pattern for how the previously derived mass balances for a multispecies chemostat can be applied to dissolved species in a multispecies biofilm. To reinforce the pattern, Equation 48 is the biofilm mass balance for biomass-associated products. It can be compared with Equation 43 for a chemostat:

$$0 = D_f \text{BAP} \frac{d^2 \text{BAP}}{dz^2} + k_{2h} X_{ah} + k_{2n} X_{an} - \frac{\hat{q}_{\text{BAP}} \text{BAP}}{K_{\text{BAP}} + \text{BAP}} X_{ah} \quad [48]$$

Biomass Species The distribution of biomass within the biofilm (e.g., $X_{ah}(z)$) is needed to solve the mass balances for the soluble species. These distributions can

be obtained in two ways. The simpler way is to specify them as model inputs. In other words, $X_{ah}(z)$, $X_{an}(z)$, and $X_i(z)$ are known in advance and held constant. Then, the model solution involves only the simultaneous solution of the mass balances for the soluble species. The substantial drawback of this simpler approach is that biomass distributions are extremely difficult to determine experimentally, and they may change with time.

Alternately, the model predicts the biomass distributions based on solving their mass-balance equations. For a slice of biofilm, the reaction terms for growth and loss are handled in a manner similar to the way the rate terms for the soluble species are handled in Equations 46 and 48. However, biomass is not transported by diffusion, since it is part of the solid matrix. Instead, biomass advects as part of a moving solid matrix. The advection of the matrix at any position in the biofilm is determined by the cumulative net growth of all biomass species from the attachment surface to the position in question.

The biomass balance is illustrated for the aerobic heterotrophs ($X_{ah}(z)$), which coexist with nitrifiers and inert biomass at some point z in the biofilm such that the total biomass density is X_f :

$$\begin{aligned} \frac{dX_{ah}(z)}{dt} = & \left[Y_h \frac{\hat{q}_h S_f}{K_h + S_f} + Y_h \frac{\hat{q}_{UAP} UAP_f}{K_{UAP} + UAP_f} \right. \\ & \left. + Y_h \frac{\hat{q}_{BAP} BAP_f}{K_{BAP} + BAP_f} - b_h - b_{\det f} - \frac{k_{2h}}{1.42} \right] X_{ah}(z) \quad \mathbf{[49]} \\ & - v_z(z) \frac{dX_{ah}(z)}{dz} - X_{ah}(z) \frac{dv_z}{dz} \end{aligned}$$

where

$$\begin{aligned} v_z(z) = & \frac{1}{X_f} \int_0^z \left\{ \left[Y_h \frac{\hat{q}_h S_f}{K_h + S_f} \right. \right. \\ & \left. + Y_h \frac{\hat{q}_{UAP} UAP_f}{K_{UAP} + UAP_f} + Y_h \frac{\hat{q}_{BAP} BAP_f}{K_{BAP} + BAP_f} - b_h - \frac{k_{2h}}{1.42} \right] X_{ah}(z) \\ & + \left[Y_n \frac{\hat{q}_h N_{1f}}{K_n + N_{1f}} - b_n - \frac{k_{2n}}{1.42} \right] X_{an}(z) \\ & \left. + (1 - f_d)[b_h X_{ah}(z) + b_n X_{an}(z)] - b_{\det f} X_f \right\} dz \quad \mathbf{[50]} \end{aligned}$$

and

$$\begin{aligned} \frac{dv_z(z)}{dz} = & \left\{ \left[Y_h \frac{\hat{q} S_f}{K + S_f} + Y_h \frac{\hat{q}_{UAP} UAP_f}{K_{UAP} + UAP_f} \right. \right. \\ & \left. + Y_h \frac{\hat{q}_{BAP} BAP_f}{K_{BAP} + BAP_f} - b_h - k \frac{k_{2h}}{1.42} \right] X_{ah}(z) \quad \mathbf{[51]} \\ & + \left[Y_n \frac{\hat{q} N_{1f}}{K_n + N_{qf}} - b_n - \frac{k_{2n}}{1.42} \right] X_{an}(z) \\ & \left. + (1 - f_d)[b_h X_{ah}(z) + b_n X_{an}(z)] - b_{\det f} X_f \right\} / X_f \end{aligned}$$

and subscript f on the soluble components refers to position z in the biofilm. The boundary condition for the attachment surface ($z = 0$) is:

$$\frac{dX_{ah}}{dz} = \frac{dX_{an}}{dz} = \frac{dX_i}{dz} = 0 \quad [52]$$

If detachment is a surface phenomenon, then $b_{det f} = 0$ for all biofilm segments except at the outer surface. For that section, $b_{det f}$ accounts for the entire detachment rate, or

$$d_{det f} = b_{det} L_f / dz \quad [53]$$

when b_{det} is the specific detachment rate averaged for the entire biofilm.

For completeness, Equations 55 and 56 give the differential mass balances for the nitrifiers ($X_{an}(z)$) and the inert biomass ($X_i(z)$):

$$\begin{aligned} \frac{dX_{an}(z)}{dt} = & \left[Y_n \frac{\hat{q}_{n1} N_{1f}}{K_{n1} + N_{1f}} - b_n - \frac{k_{2n}}{1.42} - b_{det f} \right] \\ & - v_z(z) \frac{dX_{an}(z)}{dz} - X_{an} \frac{dv_z(z)}{dz} \end{aligned} \quad [54]$$

$$\frac{dX_i(z)}{dt} = (1 - f_d)[b_h X_{ah}(z) + b_n X_{an}(z)] - v_z(z) \frac{dX_i(z)}{dz} - X_i(z) \frac{dv_z(z)}{dz} \quad [55]$$

In general, the time differentials on the left sides of Equations 49, 54, and 55 can be positive, negative, or zero. Nonzero values indicate that the relative distribution of species is changing with time. A zero value means that the segment of biofilm is at steady state with respect to species distribution.

When the value of $v_z = 0$ at the outer surface (i.e., $z = L_f$) and all accumulation terms are zero for all positions in the biofilm, the biofilm is at global steady state. These conditions for global steady state do not imply that v_x is zero at all positions within the multispecies biofilm. To the contrary, the global steady state is a dynamic one in which sections of the biofilm experiencing net positive growth export biomass to sections having net negative growth.

Figures 14 to 16 were produced from a steady-state biofilm model of the heterotroph/nitrifier/inert system described here, except that UAP and BAP were not considered. They show that the fastest growing species tend to accumulate near the outer surface, while the slower growing species accumulate more near the attachment surface, where they are protected from detachment. In the long run, slower growing species are eliminated when the detachment rate increases.

BIBLIOGRAPHY

- Furumai, H. and B. E. Rittmann (1992). "Advanced modeling of mixed populations of heterotrophs and nitrifiers considering the formation and exchange of soluble microbial products." *Water Sci. Technol.* 26(3-4), pp. 493-502.
- Furumai, H. and B. E. Rittmann (1994). "Interpretation of bacterial activities in nitrification filters by a biofilm model considering the kinetics of soluble microbial products." *Water Sci. Technol.* 30(11), pp. 147-156.

- Henze, M.; C. P. L. Grady, Jr.; W. Gujer; G. R. Marais; and T. Matsuo (1987). "Activated Sludge Model No. 1," Scientific and Technical Report No. 1., Int'l. Assoc. Water Quality, London, ISSN 10: (0-7071).
- Kissel, J. C.; P. L. McCarty; and R. L. Street (1984). "Numerical simulation of mixed-culture biofilms." *J. Environ. Engr., ASCE* 110, pp. 393–411.
- Manem, J. (1988). Interactions Between Heterotrophic and Autotrophic Bacteria in Fixed-Film Biological Processes Used in Drinking Water Treatment. Ph.D. Dissertation, Dept. of Civil Engineering, University of Illinois at Urbana-Champaign, Urbana, IL.
- Press, W. H.; B. P. Flannery; S. A. Teukolsky; and W. T. Vetterling (1986). *Numerical Recipes: The Art of Scientific Computing*. Cambridge, UK: Cambridge University Press.
- Rittmann, B. E. (1982). "Comparative performance of biofilm reactor types." *Biotechnol. Bioengr.* 24, pp. 1341–1370.
- Rittmann, B. E. and J. A. Manem (1992). "Development and experimental evaluation of a steady-state, multispecies biofilm model." *Biotechnol. Bioengr.* 39, pp. 914–922.
- Rittmann, B. E. and P. L. McCarty (1981) Substrate flux into biofilms of any thickness. *J. Environ. Engr.*
- Rittmann, B. E.; A. O. Schwarz; and P. B. Sáez (2000). "Biofilms applied to hazardous waste treatment." *Biofilms #*, J. Bryers, ed., John Wiley & Sons, Inc., pp. 207–234.
- Rittmann, B. E.; F. Trinet; D. Amar; and H. T. Chang (1992). "Measurement of the activity of a biofilm: Effects of surface loading and detachment on a three-phase, liquid-fluidized-bed reactor." *Water Sci. Technol.* 26 (3–4), pp. 585–594.
- Steeffel, C. I. and K. T. B. MacQuarrie (1996). "Approaches to modeling reactive transport in porous media." *Reviews in Mineralogy.* 34, pp. 83–130.
- Wanner, O. and W. Gujer (1986). "A multispecies biofilm model." *Biotechnol. Bioengr.* 28, pp. 314–328.
- Watanabe, Y.; S. Okabe; K. Hirata; and S. Masuda (1995). "Simultaneous removal of organic materials and nitrogen by micro-aerobic biofilms. *Water Sci. Technol.* 31(1), pp. 170–177.
- Woolschlager, J. and B. E. Rittmann (1995). "Evaluating what is measured by BDOC and AOC Tests." *Review Science de l'Eau.* 8, pp. 371–385.